Nonlinear and Adaptive Backstepping Designs for Tracking Control of Ships

J.-M. Godhavn, T. I. Fossen and S. P. Berge

Revised version: Special Issue on Marine Systems Control, International Journal of Adaptive Control and Signal Processing

July 30, 1998

Abstract

In this paper two nonlinear control laws for ships are derived by using a nonlinear ship model which includes the hydrodynamic effects due to time-varying speed and wave frequency. The nonlinear ship model does not have the structural properties of symmetric inertia and positive damping at high speed, which are common assumptions, when designing nonlinear ship tracking control systems. Backstepping control designs are used to circumvent the problem of a non-symmetrical inertia matrix. The first case is ship tracking with full actuation in surge, sway and yaw while the second case discusses an emergency situation where a ship is supposed to track a time-varying trajectory by using the bow thruster and one of the main propellers as actuation devices only. The application of speed and wave dependent models for ship control is a first step towards the design of a new generation of nonlinear ship control systems that can operate under time-varying speed and wave frequency conditions. Previous work has often relied on the assumption of constant speed, and practical solutions have been based on switching between different control schemes at different speeds. Slowly-varying environmental disturbances, such as ocean current, 2nd-order wave-induced disturbances and wind forces, are compensated for by using adaptive backstepping. Global uniform asymptotic stability (GUAS) is proven for the fully actuated case by using a recent theorem for GUAS when backstepping with integral action, whereas asymptotic tracking of position and velocity are shown for the degraded control case. Computer simulations illustrate the performance and the robustness of the control laws for an offshore supply vessel.

1 Introduction

Two nonlinear backstepping control laws for ship tracking control are derived in this paper. The first one discusses tracking of overactuated ships, whereas the second control law is intended for emergency situations, where the number of available controls is reduced. This is a first attempt towards the design of nonlinear ship control systems incorporating the effects of time-varying speed. Hence, look-up tables and gain-scheduling techniques can be avoided, when designing ship control systems at different speeds. The main contributions of the paper are two control laws for *fully* and *degraded* control of ships, which can operate at all forward speeds. Global uniform asymptotic stability (GUAS) is proven for the fully actuated case by applying the results of Krstic et al. [13], Krstic [14], and a recent theorem for GUAS when backstepping with integral action by Fossen and Teel [5]. The second control law is shown to give convergence in position and velocity to any smooth desired trajectory, whereas the orientation is not controlled directly. Both control laws

have also the feature of compensating for slowly varying environmental disturbances such as wind, wave drift, and water current.

Most nonlinear ship control systems are based on the assumption that the inertia matrix including hydrodynamic added inertia is symmetrical, independent of speed and constant by assuming ideal fluid (potential theory) and that the coefficients are independent of the wave frequency. Similarly, it is common to assume that the damping matrix is independent of the speed and the wave frequency and with little or no structural properties. These are good assumptions for station-keeping and low-speed applications like dynamic positioning (DP) of ships, Fossen [2]. A ship moving at non-zero forward speed can, however, not be described by symmetrical inertia and damping matrices. This has been shown by Salvesen, Tuck and Faltinsen [16]. The work of [16] has been reformulated in a vectorial setting by Berge and Fossen [1] in order to exploit structural properties like symmetry, skew-symmetry, positiveness and dissipativity of the ambient water-vessel system. The derivation of the marine vehicle equations of motion in 6 degrees of freedom (DOF) with focus on skew-symmetrical parameterizations of Coriolis and centripetal forces including hydrodynamic added mass terms are discussed by Fossen and Fjellstad [3], while a more general text on 6 DOF nonlinear modelling of marine vehicles is found in Fossen [2].

For ships with only two controls, nonlinear tracking control with a simplified dynamic model has been discussed by Godhavn [10] and [11]. Vik and Fossen [18] and Husa and Fossen [12] discussed tracking at constant speed. DP applications at *low-speed* have been discussed by Fossen and Grøvlen [9].

All results in this paper are based on full state feedback from position, heading, velocity and angular rate. These measurements are, however, available from relatively inexpensive measurement devices based on GPS/INS, that is the satellite-based Global Positioning System (GPS) aided with an inertial navigation system (INS) using strapdown motion sensors like gyroscopes and accelerometers. In the case when only position and yaw angle measurements are available, the velocities can be estimated using the passive nonlinear observer of Fossen and Strand [6] or by using the observer backstepping approach of Fossen and Grøvlen [9]. Both these approaches rely on the assumption of linear damping and negligible Coriolis and centripetal terms.

Environmental disturbances as well as measurement noise are important issues in ship control. Slowly-varying disturbances like 2nd-order wave drift, ocean currents and wind are compensated for in this paper by using parameter adaptation. In addition, it is assumed that measurement noise and 1st-order wave disturbances are properly filtered (wave filtering) in order to avoid wear and tear of the actuation devices and to prevent noise from entering the feedback control loop, see Fossen [2]. The slowly-varying disturbances are lumped together in an unknown bias term, which is estimated by using the technique of adaptive backstepping.

The paper is outlined as follows: Section 2 is a brief review of the nonlinear speed dependent model of Berge and Fossen [1], Section 3 discusses nonlinear overactuated backstepping tracking control, whereas Section 4 describes a control law that can be used for way-point tracking of a supply vessel with only two controls. Finally, Section 5 gives the conclusions.

2 Ship Model

2.1 Kinematic Model

For most ships it is common to reduce the general 6 DOF model to motion in surge, sway, and yaw only. This is done by neglecting the heave, roll and pitch modes which are open loop stable for most ships. The state vector $\boldsymbol{\eta} \in \mathrm{SE}(2)$ is defined by:

$$\boldsymbol{\eta} = [x, y, \psi]^T \tag{1}$$

where $(x, y) \in \Re^2$ is the position of the ship given in an inertial frame (e.g. North, East from some point of reference), and $\psi \in [0, 2\pi\rangle$ is the heading angle of the ship relative to e.g. geographic North. The kinematics is written:

$$\dot{\boldsymbol{\eta}} = \mathbf{R}(\psi)\boldsymbol{\nu} \tag{2}$$

where $\mathbf{R}$ is the rotation matrix in yaw and $\boldsymbol{\nu} \in \Re^3$ is a vector containing the linear body-fixed velocities. $\mathbf{R}$ is defined as:

$$\mathbf{R}(\psi) = \begin{bmatrix} \cos\psi & -\sin\psi & 0 \\ \sin\psi & \cos\psi & 0 \\ 0 & 0 & 1 \end{bmatrix} \tag{3}$$

with the property $\mathbf{R}^T = \mathbf{R}^{-1}$. The velocity vector is $\boldsymbol{\nu}$ is defined by:

$$\boldsymbol{\nu} = [u, v, r]^T . \tag{4}$$

Here u is forward velocity (surge), v is transverse velocity (sway), and r is the angular velocity in yaw (rate of turn).

2.2 Dynamic Model

The nonlinear ship model used in this paper is based on Berge and Fossen [1] and Fossen and Fjellstad [3]. The model describes the motion of a ship in surge, sway and yaw. The ship speed $U = \sqrt{u^2 + v^2} \geq 0$ and frequency of encounter ω_e are included to describe the change in dynamics according to time-varying speed and wave frequencies.

Frequency of Encounter

Let the angle β denote the heading of the ship relative to the waves such that $\beta = 0$ in following seas and $\beta = \pi$ in ahead seas. For a ship moving at forward speed U the wave frequency ω_0 (peak frequency of the wave spectrum) is modified according to:

$$\omega_e = \omega_0 - \frac{\omega_0^2}{g} U \cos\beta \tag{5}$$

where g is the gravity constant ($9.8\, m/s^2$) and ω_e is denoted the *frequency of encounter*.

Ship Dynamics

Denote the control forces in surge and sway, and the yaw moment by $\boldsymbol{\tau}$. The nonlinear ship model is given by:

$$\mathbf{M}(U)\dot{\boldsymbol{\nu}} + \mathbf{n}(\boldsymbol{\nu}, U) = \boldsymbol{\tau} \tag{6}$$

where $\mathbf{M}$, the matrix of inertia, is assumed invertible, and $\mathbf{n}$ is a vector including the Coriolis and centripetal forces ($\mathbf{C}(\boldsymbol{\nu})\boldsymbol{\nu}$) and the damping forces ($\mathbf{D}(\boldsymbol{\nu}, U)\boldsymbol{\nu}$), that is:

$$\mathbf{n}(\boldsymbol{\nu}, U) = \mathbf{C}(\boldsymbol{\nu})\boldsymbol{\nu} + \mathbf{D}(\boldsymbol{\nu}, U)\boldsymbol{\nu} \tag{7}$$

In this paper the following inertia matrix is considered

$$\mathbf{M}(U) = \mathbf{M}_{RB} + \mathbf{M}_A(U) \tag{8}$$

together with this Coriolis matrix

$$\mathbf{C}(\boldsymbol{\nu}) = \mathbf{C}_{RB}(\boldsymbol{\nu}) + \mathbf{C}_A(\boldsymbol{\nu}) \tag{9}$$

Here the subscripts denote RB (rigid-body) and A (hydrodynamic added mass), see Fossen [2] for details. The hydrodynamic added inertia matrix $\mathbf{M}_A$ is modelled as a sum of three parts

$$\mathbf{M}_A(U) = \mathbf{M}_{A0} + \mathbf{M}_{A1}(U) + \mathbf{M}_{A2}(U) \tag{10}$$

where $\mathbf{M}_{A0}$ is constant, $\mathbf{M}_{A1}$ has terms proportional to U/ω_e^2, and $\mathbf{M}_{A2}$ has terms proportional to U^2/ω_e^2. The resulting inertia matrix depends on both the speed U and the frequency of encounter ω_e. It is assumed that $\omega_e \neq 0$. Damping is modelled by potential damping and quadratic damping

$$\mathbf{D}(\boldsymbol{\nu}, U) = \mathbf{D}_P(U) + \mathbf{D}_M(\boldsymbol{\nu})$$

The potential damping matrix $\mathbf{D}_P(U)$ takes the same form as the added inertia:

$$\mathbf{D}_P(U) = \mathbf{D}_{P0} + \mathbf{D}_{P1}(U) + \mathbf{D}_{P2}(U) \tag{11}$$

where $\mathbf{D}_{P0}$ is constant, $\mathbf{D}_{P1}$ has terms proportional to U, and $\mathbf{D}_{P2}$ has terms proportional to U^2/ω_e^2. Quadratic damping $\mathbf{D}_M(\boldsymbol{\nu})\boldsymbol{\nu}$ (vortex shedding as modelled by Morison's equation) is modelled by terms like $u\,|u|, v\,|v|, v\,|r|$, etc. Other types of damping forces like $\mathbf{D}_W(\boldsymbol{\nu},U)\boldsymbol{\nu}$ (wave drift damping), and $\mathbf{D}_S(\boldsymbol{\nu},U)\boldsymbol{\nu}$ (skin friction) can be included without loss of generality, see Berge and Fossen [1]. The parameters can be found by system identification and maneuvering trials with a full-scale vessel. They can also be found analytically or by performing experiments in a towing tank, for instance.

2.3 Environmental Disturbances

Constant or slowly-varying environmental disturbances due to ocean currents, 2nd-order wave drift and wind can be compensated for by using adaptive backstepping. The environmental disturbances $\mathbf{e}$ are usually modelled as a constant (or slowly-varying) force with respect to the inertial reference frame, that is:

$$\dot{\mathbf{e}} = \mathbf{0}$$

Hence, the body-fixed environmental force $\mathbf{R}^T(\psi)\mathbf{e}$ can be added to the ship dynamics according to:

$$\mathbf{M}\,(U)\,\dot{\boldsymbol{\nu}} + \mathbf{n}\,(\boldsymbol{\nu},U) = \boldsymbol{\tau} + \mathbf{R}^T(\psi)\mathbf{e}. \tag{12}$$

2.4 Speed Dependent Actuator Model

The control forces and moments $\boldsymbol{\tau} \in \Re^3$ can be written:

$$\boldsymbol{\tau} = \mathbf{T}\mathbf{K}(U)\mathbf{u} \tag{13}$$

where $\mathbf{T} \in \Re^{3\times m}$ is the thruster/rudder configuration matrix and $\mathbf{K}(U) \in \Re^{m\times m}$ is a diagonal matrix of speed dependent force coefficients. The control input vector is denoted by $\mathbf{u} \in \Re^m$. The ship is said to be *overactuated* if $m > 3$. The matrix $\mathbf{T}$ will only depend on the location of the

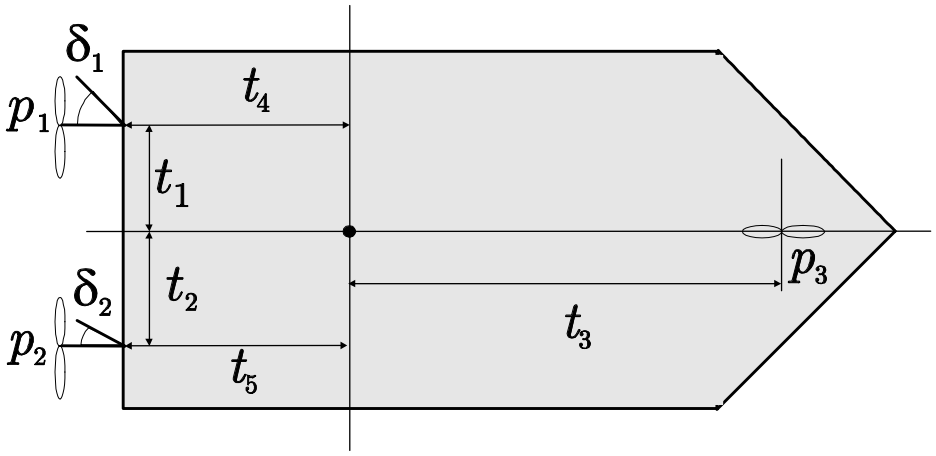

Figure 1: The figure shows the actuator configuration for the class of ships considered in this paper.

actuators. For a ship with two main propellers aft, one tunnel thruster in the bow and two rudders aft of the ship, $\mathbf{T}$, $\mathbf{K}$, and $\mathbf{u}$ are given by

$$\begin{aligned}
\mathbf{T} &= \begin{bmatrix} 1 & 1 & 0 & 0 & 0 \\ 0 & 0 & 1 & -1 & -1 \\ t_1 & t_2 & t_3 & t_4 & t_5 \end{bmatrix} && \begin{matrix} \text{(surge)} \\ \text{(sway)} \\ \text{(yaw)} \end{matrix} \\
\mathbf{K}(U) &= \begin{bmatrix} k_1 & 0 & 0 & 0 & 0 \\ 0 & k_2 & 0 & 0 & 0 \\ 0 & 0 & k_3 e^{-aU^2} & 0 & 0 \\ 0 & 0 & 0 & k_4 U^2 & 0 \\ 0 & 0 & 0 & 0 & k_5 U^2 \end{bmatrix} && \begin{matrix} \text{(aft main propeller \#1)} \\ \text{(aft main propeller \#2)} \\ \text{(bow tunnel thruster \#1)} \\ \text{(rudder \#1)} \\ \text{(rudder \#2)} \end{matrix} \\
\mathbf{u} &= \left[p_1 \left| p_1 \right|, p_2 \left| p_2 \right|, p_3 \left| p_3 \right|, \delta_1, \delta_2 \right]^T
\end{aligned}$$

Here p_i $(i = 1...3)$ denote the propeller pitch ratios (or propeller revolutions for fixed blade propellers) and δ_i $(i = 1...2)$ are the rudder angles. The expression for $\mathbf{K}(U)$ can be modified to include state dependent expressions due to 4-quadrant open water tests and propeller losses due to hydrodynamic effects like cross-flows, thruster interactions, suction, cavitation etc. The moment arms t_i $(i = 1...5)$ are given by the location of the actuators. The force coefficients k_i $(i = 1...5)$ depend on the type of actuator considered. Notice that the rudder forces $k_4 U^2 = k_5 U^2 = 0$ for $U = 0$. Hence, station-keeping (dynamic positioning) can only be obtained by means of the two aft propellers and the tunnel thruster. During cruise $(U > 0)$ all actuators can be used. However, the tunnel (transverse) thruster force will drop with a factor of e^{-aU^2} to take care of the effect due to increased water speed around the hull. The control allocation algorithm must be able to deal with varying speed U and time-varying control configurations e.g. the transition from a overactuated control configuration to a control configuration with fewer controls than degrees of freedom (DOF). At zero speed the model reduces to dynamic positioning by means of p_1, p_2 and p_3. Moreover:

$$\begin{aligned}
\boldsymbol{\tau} &= \begin{bmatrix} k_1 & k_2 & 0 \\ 0 & 0 & k_3 \\ t_1 k_1 & t_2 k_2 & t_3 k_3 \end{bmatrix} \begin{bmatrix} p_1 \left| p_1 \right| \\ p_2 \left| p_2 \right| \\ p_3 \left| p_3 \right| \end{bmatrix} \\
&= \mathbf{B}_{DP} \mathbf{u}
\end{aligned} \tag{14}$$

where the matrix $\mathbf{B}_{DP} \in \Re^{3\times 3}$ is square and non-singular for $t_1 \neq t_2$. This will be the case for all ships with two main propellers since they are located symmetrical about the ship centerline that is $t_2 = -t_1$. From (14) it is seen that the tunnel thruster can be used to produce sway motion, while the main propellers are used to produce surge and yaw motions. This is the typical configuration for zero speed. The weighted pseudo inverse of the matrix $\mathbf{B} = \mathbf{TK}$ is applied in the speed dependent control allocation for the overactuated case. This is the topic for the next section.

2.5 Speed Dependent Control Allocation

The optimal control input vector $\mathbf{u}$ in the *overactuated* case is derived from a desired control force $\boldsymbol{\tau}$ by minimizing the following criterion with respect to $\mathbf{u}$:

$$J = \frac{1}{2}(\boldsymbol{\tau} - \mathbf{B}(U)\mathbf{u})^T \mathbf{W}(U)(\boldsymbol{\tau} - \mathbf{B}(U)\mathbf{u}) \tag{15}$$

where the weight matrix is diagonal $\mathbf{W}(U)$ =diag$\{w_1(U), w_2(U), ..., w_n(U)\}$. This results in the following relationship between the control input vector $\mathbf{u}$ and the desired generalized control force $\boldsymbol{\tau}$ (to be derived in Section 3)

$$\mathbf{u} = \mathbf{B}_W^{\dagger}(U)\boldsymbol{\tau} \tag{16}$$

where the weighted pseudo-inverse $\mathbf{B}_W^{\dagger}$ is given by

$$\mathbf{B}_W^{\dagger}(U) = \mathbf{W}^{-1}(U)\mathbf{B}^T(\mathbf{B}\mathbf{W}^{-1}(U)\mathbf{B}^T)^{-1} \tag{17}$$

The transition between station-keeping (zero speed) and cruise (constant speed) implies that the number of available actuators is changed (reconfigurable control). For instance, this can be done by defining:

$$\mathbf{W}(U) = \text{diag}\left\{1, 1, \frac{1}{2}b_1(1 + e^{b_2 U^2}), b_3 + b_4 \exp\left(\frac{1}{\epsilon + U}\right), b_3 + b_4 \exp\left(\frac{1}{\epsilon + U}\right)\right\} \tag{18}$$

where ϵ is a small positive number used to avoid numerical difficulties at zero speed and $b_i (i = 1...4)$ are positive design parameters. The weight matrix $\mathbf{W}(U)$ reflects that it is expensive to use rudders at zero speed compared to thrust. For higher speeds, the price of the tunnel thruster increases whereas the rudders become more inexpensive.

3 Overactuated Control

In this section the recursive backstepping method of Krstic et al. [13] and Fossen and Berge [8] will be applied to derive control laws for ships operating at all speeds including dynamic positioning applications. It is assumed that the actuators can produce generalized forces in all 3 degrees of freedom (surge, sway, and yaw). The control law is able to counteract environmental disturbances by using *constant parameter adaptation*, Fossen and Teel [5]. The tracking error is defined as:

$$\mathbf{z}_1 = \boldsymbol{\eta} - \boldsymbol{\eta}_d \tag{19}$$

where $\boldsymbol{\eta}_d$ is the desired state in an inertial frame (e.g. North-East position and heading angle). The desired state $\boldsymbol{\eta}_d$ is a smooth function of time. It can be generated as an interpolation of given way-points by using a route planner, see Godhavn [10] for instance. The first step of backstepping is the definition of a Lyapunov function candidate (LFC):

$$V_1 = \frac{1}{2}\mathbf{z}_1^T \mathbf{P}_1 \mathbf{z}_1 \tag{20}$$

where $\mathbf{P}_1 = \mathbf{P}_1^T > 0$ (positive definite) is a design parameter matrix. The time derivative along the trajectories of V_1 is given by

$$\dot{V}_1 = \mathbf{z}_1^T \mathbf{P}_1 (\mathbf{R}\boldsymbol{\nu} - \dot{\boldsymbol{\eta}}_d) \triangleq -\mathbf{z}_1^T \mathbf{C}_1 \mathbf{z}_1 + \mathbf{z}_1^T \mathbf{z}_2 \tag{21}$$

Here $\mathbf{C}_1 = \mathbf{C}_1^T > 0$ is a design matrix, and the second backstepping variable $\mathbf{z}_2$ is defined by:

$$\mathbf{z}_2 = \mathbf{C}_1 \mathbf{z}_1 + \mathbf{P}_1 (\mathbf{R}\boldsymbol{\nu} - \dot{\boldsymbol{\eta}}_d) \tag{22}$$

The estimate of the environmental force $\mathbf{e}$ is denoted $\hat{\mathbf{e}}$, and the parameter estimation error is written $\tilde{\mathbf{e}} = \hat{\mathbf{e}} - \mathbf{e}$. Define a second quadratic LFC by

$$V_2 = V_1 + \frac{1}{2}\mathbf{z}_2^T \mathbf{P}_2 \mathbf{z}_2 + \frac{1}{2}\tilde{\mathbf{e}}^T \boldsymbol{\Gamma}^{-1} \tilde{\mathbf{e}} \; > 0 \tag{23}$$

where $\mathbf{P}_2 = \mathbf{P}_2^T > 0$ and $\boldsymbol{\Gamma} = \boldsymbol{\Gamma}^T > 0$ are two design matrices. Differentiation of V_2 along the trajectories of $\mathbf{z}$ and $\tilde{\mathbf{e}}$, yields:

$$\begin{aligned} \dot{V}_2 &= -\mathbf{z}_1^T \mathbf{C}_1 \mathbf{z}_1 + \tilde{\mathbf{e}}^T \boldsymbol{\Gamma}^{-1} \dot{\hat{\mathbf{e}}} \\ &\quad + \mathbf{z}_2^T \left(\mathbf{z}_1 + \mathbf{P}_2 \mathbf{C}_1 \dot{\mathbf{z}}_1 + \mathbf{P}_2 \mathbf{P}_1 \left(\dot{\mathbf{R}}\boldsymbol{\nu} - \ddot{\boldsymbol{\eta}}_d \right) \right) \\ &\quad + \mathbf{z}_2^T \mathbf{P}_2 \mathbf{P}_1 \mathbf{R} \mathbf{M}^{-1}(U) \left(\boldsymbol{\tau} - \mathbf{n}(\boldsymbol{\nu}, U) + \mathbf{R}^T \mathbf{e} \right) \end{aligned} \tag{24}$$

Collecting terms in $\tilde{\mathbf{e}}$, yields:

$$\begin{aligned} \dot{V}_2 &= -\mathbf{z}_1^T \mathbf{C}_1 \mathbf{z}_1 + \tilde{\mathbf{e}}^T \boldsymbol{\Gamma}^{-1} (\dot{\hat{\mathbf{e}}} - \boldsymbol{\Gamma} \mathbf{R} \mathbf{M}^{-T}(U) \mathbf{R}^T \mathbf{P}_1 \mathbf{P}_2 \mathbf{z}_2) \\ &\quad + \mathbf{z}_2^T \left(\mathbf{z}_1 + \mathbf{P}_2 \mathbf{C}_1 \dot{\mathbf{z}}_1 + \mathbf{P}_2 \mathbf{P}_1 \left(\dot{\mathbf{R}}\boldsymbol{\nu} - \ddot{\boldsymbol{\eta}}_d \right) \right) \\ &\quad + \mathbf{z}_2^T \mathbf{P}_2 \mathbf{P}_1 \mathbf{R} \mathbf{M}^{-1}(U) \left(\boldsymbol{\tau} - \mathbf{n}(\boldsymbol{\nu}, U) + \mathbf{R}^T \hat{\mathbf{e}} \right) \end{aligned} \tag{25}$$

The parameter adaptation law

$$\dot{\hat{\mathbf{e}}} = \boldsymbol{\Gamma} \mathbf{R} \mathbf{M}^{-T}(U) \mathbf{R}^T \mathbf{P}_1 \mathbf{P}_2 \mathbf{z}_2 \tag{26}$$

makes the second term of (25) zero. The control force

$$\begin{aligned} \boldsymbol{\tau} &= \mathbf{n}(\boldsymbol{\nu}, U) - \mathbf{R}^T \hat{\mathbf{e}} - \mathbf{M}(U) \mathbf{R}^T (\dot{\mathbf{R}}\boldsymbol{\nu} - \ddot{\boldsymbol{\eta}}_d) \\ &\quad - \mathbf{M}(U) \mathbf{R}^T \mathbf{P}_1^{-1} \left(\mathbf{C}_1 \dot{\mathbf{z}}_1 + \mathbf{P}_2^{-1} (\mathbf{z}_1 + \mathbf{C}_2 \mathbf{z}_2) \right) \end{aligned} \tag{27}$$

where $\mathbf{C}_2 = \mathbf{C}_2^T > 0$ is a positive definite design matrix, finally yields V_2 non-positive by

$$\dot{V}_2 = -\mathbf{z}_1^T \mathbf{C}_1 \mathbf{z}_1 - \mathbf{z}_2^T \mathbf{C}_2 \mathbf{z}_2 \leq 0 \tag{28}$$

The speed dependent control allocation algorithm (16)–(17), gives a 5-vector of control inputs $\mathbf{u}$ from (27), which in the case of zero speed ($U = 0$) reduces to (14).

Theorem 1 (Globally Uniformly Asymptotically Stable Tracking Control Law) *The equilibrium point* $(\mathbf{z}_1, \mathbf{z}_2, \tilde{\mathbf{e}}) = (\mathbf{0}, \mathbf{0}, \mathbf{0})$ *of the nonlinear system (12) and (13) with control law (27), control allocation algorithm (16), and disturbance adaptation law (26) is GUAS for smooth reference trajectories* $\boldsymbol{\eta}_d, \dot{\boldsymbol{\eta}}_d, \ddot{\boldsymbol{\eta}}_d \in L_\infty$. *Tracking is achieved of both position and heading, since* $\mathbf{z}_1 = \boldsymbol{\eta} - \boldsymbol{\eta}_d \to \mathbf{0}$, *and velocity and yaw rate, since* $\mathbf{z}_2 = \mathbf{C}_1 \mathbf{z}_1 + \mathbf{P}_1 (\mathbf{R}\boldsymbol{\nu} - \dot{\boldsymbol{\eta}}_d) \to \mathbf{0}$ *implies that* $\dot{\boldsymbol{\eta}} - \dot{\boldsymbol{\eta}}_d \to \mathbf{0}$.

Proof. The proof is based on Fossen and Teel [5]. The error dynamics can be written:

$$\begin{bmatrix} \dot{\mathbf{z}}_1 \\ \dot{\mathbf{z}}_2 \end{bmatrix} = -\begin{bmatrix} \mathbf{P}_1^{-1}\mathbf{C}_1 & -\mathbf{P}_1^{-1} \\ \mathbf{P}_2^{-1} & \mathbf{P}_2^{-1}\mathbf{C}_2 \end{bmatrix} \begin{bmatrix} \mathbf{z}_1 \\ \mathbf{z}_2 \end{bmatrix} + \begin{bmatrix} \mathbf{0} \\ -\mathbf{P}_1\mathbf{R}\mathbf{M}^{-1}(U)\mathbf{R}^T \end{bmatrix} \tilde{\mathbf{e}} \tag{29}$$

$$\dot{\tilde{\mathbf{e}}} = -\mathbf{\Gamma}\mathbf{R}\mathbf{M}^{-T}(U)\mathbf{R}^T\mathbf{P}_1\mathbf{P}_2\mathbf{z}_2 \tag{30}$$

Stability is established, since $V_2 > 0$ (23) and $\dot{V}_2 \leq 0$ (25). Then $\mathbf{z}_1$, $\mathbf{z}_2$, and $\tilde{\mathbf{e}}$ are bounded. The error dynamics is non-autonomous since the inertia matrix depends on the speed U, which again depends on both the error variables $\mathbf{z}_1$ and $\mathbf{z}_2$, and the time-varying desired trajectory $\boldsymbol{\eta}_d(t)$. Hence, LaSalle's theorem for invariant manifolds cannot be used. Global attractivity is proven by using the theorem of Fossen and Teel [5], requiring that $\mathbf{B}^T\mathbf{B}$ is invertible with:

$$\mathbf{B} = \begin{bmatrix} \mathbf{0} \\ -\mathbf{P}_1\mathbf{R}\mathbf{M}^{-1}(U)\mathbf{R}^T \end{bmatrix} \tag{31}$$

This requirement is clearly satisfied, since the regressor matrix is always invertible with $\text{rank}(\mathbf{P}_1\mathbf{R}\mathbf{M}^{-1}(U)\mathbf{R}^T) = 3$. Hence, it may be concluded that the resulting system is GUAS.

Remark 1 (Globally Asymptotically Stable DP Regulator) *If $\boldsymbol{\eta}_d$ =constant (set-point regulation) the error dynamics (29)–(30) becomes autonomous. Hence, GAS follows directly by application of LaSalle's theorem for invariant manifolds, see Krstic [14] for details.*

3.1 Case Study: Supply Vessel

The control law was simulated on a model of a supply vessel with parameters given in Appendix A. Non-dimensional model parameters were used in accordance to the *Bis scaling* system, see Fossen [2]. The *non-dimensional* design parameters were selected by trial and failure. This resulted in $\mathbf{P}_1'' = 10 \cdot \mathbf{I}$, $\mathbf{P}_2'' = \mathbf{I}$, $\mathbf{C}_1'' = \mathbf{C}_2'' = \mathbf{I}, \mathbf{\Gamma}''=10^{-3} \cdot \mathbf{I}$. The disturbance was selected as $\mathbf{e}''=5 \cdot 10^4[0, 1/mg, 0]^T$. A smooth trajectory looking like the number 8 with desired forward speed $2.5\,m/s$ was generated from a set of way points and a second order filter. The time responses with sampling time $\Delta = 0.2s$ are shown in Figures 2-6. It is seen that the position and the heading of the ship track the desired trajectory well. The estimated enviromental disturbances converge to the true values. The rapid changes of the inputs can be reduced by including a model of the actuator dynamics in the control design, see Fossen and Berge [8].

4 Degraded control

The control algorithm in Section 3 is intended for overactuated ships. In this section a scenario where 3 of the actuation devices fail is discussed, such that only 2 control actuators are available to control the surge, sway and yaw modes. It will be assumed that only one of the main propellers is operative. In addition to this, it is assumed that the tunnel thruster in the bow can be used even though the thrust from the tunnel thruster will decrease significantly with the speed of the ship. Both the rudders are assumed to be out of order. The ship is, however, controllable, even though it is has fewer controls than DOF. Consider the actuator model presented in Section 2.4, which with $p_2 = \delta_1 = \delta_2 = 0$ reduces to:

$$\begin{aligned} \boldsymbol{\tau} &= \begin{bmatrix} k_1 & 0 \\ 0 & k_3 e^{-aU^2} \\ t_1 k_1 & t_3 k_3 e^{-aU^2} \end{bmatrix} \begin{bmatrix} p_1 \, |p_1| \\ p_3 \, |p_3| \end{bmatrix} \\ &= \mathbf{B}_{TR}\mathbf{u}. \end{aligned} \tag{32}$$

Notice that the aft propeller is used to control the surge mode, while the tunnel thruster is used to control the sway mode. With only two available linearly independent controls, it is impossible to independently control all three degrees of freedom simultaneously. However, it is possible to design a controller which gives convergence of position directly, and only indirectly the heading angle by using the approach of Fossen, Godhavn, Berge, and Lindegaard [7]. The orientation of the ship, the heading angle ψ, is controlled indirectly. This approach relies on the following Conjecture:

Conjecture 2 (Stable zero dynamics in yaw) *The zero dynamics in yaw for the nonlinear system (12) and (32) is stable.*

The physical reasoning for Conjecture 2 is that course stable ships are well damped in yaw. The damping terms increase with increasing yaw rate r, and will constrain the yaw rate for bounded inputs $\tau_3 = t_1\tau_1 + t_3\tau_2$. Whether this conjecture is true or not, must be checked for each ship model. It will also depend on the thrusters and the desired trajectory.

Design of Backstepping Control Law

Define the position tracking error:

$$\mathbf{z}_1 = \mathbf{p} - \mathbf{p}_d \tag{33}$$

where $\mathbf{p}_d$ is the desired position. The position $\mathbf{p}$ is a projection of the state $\boldsymbol{\eta}$ by

$$\mathbf{p} = \begin{bmatrix} x \\ y \end{bmatrix} \triangleq \boldsymbol{\Pi}\boldsymbol{\eta} \tag{34}$$

where $\boldsymbol{\Pi}$ is a projection matrix:

$$\boldsymbol{\Pi} = \begin{bmatrix} 1 & 0 & 0 \\ 0 & 1 & 0 \end{bmatrix} \tag{35}$$

The kinematics is reduced to:

$$\dot{\mathbf{p}} = \boldsymbol{\Pi}\mathbf{R}\boldsymbol{\nu}$$

The backstepping design starts with the following LFC:

$$V_1 = \frac{1}{2}\mathbf{z}_1^T\mathbf{P}_1\mathbf{z}_1 \tag{36}$$

where $\mathbf{P}_1 = \mathbf{P}_1^T > 0$ is a design matrix. The time derivative of (36) along the system trajectories is given by

$$\dot{V}_1 = \mathbf{z}_1^T\mathbf{P}_1\left(\boldsymbol{\Pi}\mathbf{R}\boldsymbol{\nu} - \dot{\mathbf{p}}_d\right) \triangleq -\mathbf{z}_1^T\mathbf{C}_1\mathbf{z}_1 + \mathbf{z}_1^T\mathbf{z}_2 \tag{37}$$

where the new backstepping variable $\mathbf{z}_2$ is defined as:

$$\mathbf{z}_2 = \mathbf{C}_1\mathbf{z}_1 + \mathbf{P}_1(\boldsymbol{\Pi}\mathbf{R}\boldsymbol{\nu} - \dot{\mathbf{p}}_d) \tag{38}$$

with $\mathbf{C}_1 = \mathbf{C}_1^T > 0$ being another design matrix. Let $\tilde{\mathbf{e}} = \hat{\mathbf{e}} - \mathbf{e}$ be the parameter estimation error and define another positive definite LFC:

$$V_2 = V_1 + \frac{1}{2}\mathbf{z}_2^T\mathbf{P}_2\mathbf{z}_2 + \frac{1}{2}\tilde{\mathbf{e}}^T\boldsymbol{\Gamma}^{-1}\tilde{\mathbf{e}} \tag{39}$$

The time derivative of V_2 along the system trajectories is given by

$$\begin{aligned} \dot{V}_2 \;=\; & -\mathbf{z}_1^T\mathbf{C}_1\mathbf{z}_1 + \tilde{\mathbf{e}}^T\boldsymbol{\Gamma}^{-1}\dot{\hat{\mathbf{e}}} \\ & + \mathbf{z}_2^T\left(\mathbf{z}_1 + \mathbf{P}_2\mathbf{C}_1\left(\boldsymbol{\Pi}\mathbf{R}\boldsymbol{\nu} - \dot{\mathbf{p}}_d\right)\right) \\ & + \mathbf{z}_2^T\mathbf{P}_2\mathbf{P}_1\left(\boldsymbol{\Pi}\dot{\mathbf{R}}\boldsymbol{\nu} - \ddot{\mathbf{p}}_d + \boldsymbol{\Pi}\mathbf{R}\mathbf{M}^{-1}\left(U\right)\left(\boldsymbol{\tau} - \mathbf{n}\left(\boldsymbol{\nu}\right) + \mathbf{R}^T\mathbf{e}\right)\right) \end{aligned} \tag{40}$$

Choosing the parameter adaptation law:

$$\dot{\hat{\mathbf{e}}} = \mathbf{\Gamma R M}^{-T}(U)\mathbf{R}^T\mathbf{\Pi}^T\mathbf{P}_1\mathbf{P}_2\mathbf{z}_2 \tag{41}$$

yields:

$$\begin{aligned}\dot{V}_2 &= -\mathbf{z}_1^T\mathbf{C}_1\mathbf{z}_1+\mathbf{z}_2^T(\mathbf{z}_1+\mathbf{P}_2\mathbf{C}_1(\mathbf{\Pi R}\boldsymbol{\nu}-\dot{\mathbf{p}}_d)) \\ &\quad +\mathbf{z}_2^T\mathbf{P}_2\mathbf{P}_1\left(\mathbf{\Pi}\dot{\mathbf{R}}\boldsymbol{\nu}-\ddot{\mathbf{p}}_d+\mathbf{R}_\pi\mathbf{\Pi M}^{-1}(U)\left(\boldsymbol{\tau}-\mathbf{n}(\boldsymbol{\nu})+\mathbf{R}^T\hat{\mathbf{e}}\right)\right)\end{aligned} \tag{42}$$

where the property $\mathbf{\Pi R} = \mathbf{R}_\pi\mathbf{\Pi}$ has been applied with:

$$\mathbf{R}_\pi = \begin{bmatrix} \cos\psi & -\sin\psi \\ \sin\psi & \cos\psi \end{bmatrix}$$

Define a smooth mapping of the input $\mathbf{u}$ to a new equivalent input vector $\mathbf{f}$ by:

$$\begin{aligned}\mathbf{f} &= \mathbf{f}(\boldsymbol{\tau}(\mathbf{u})) \\ &= \mathbf{\Pi M}^{-1}\left(\boldsymbol{\tau}(\mathbf{u})-\mathbf{n}(\boldsymbol{\nu})+\mathbf{R}^T\hat{\mathbf{e}}\right) \\ &= \left(\mathbf{\Pi M}^{-1}\mathbf{B}\right)\mathbf{u}+\mathbf{\Pi M}^{-1}(\mathbf{R}^T\hat{\mathbf{e}}-\mathbf{n}(\boldsymbol{\nu})) \\ &= \mathbf{B}_f\mathbf{u}+\mathbf{n}_f(\boldsymbol{\nu})\end{aligned} \tag{43}$$

where

$$\begin{aligned}\mathbf{B}_f &= \mathbf{\Pi M}^{-1}\mathbf{B} \\ &= \begin{bmatrix} \frac{1}{m_{11}} & 0 & 0 \\ 0 & \frac{-m_{33}}{m_{22}m_{33}-m_{23}m_{32}} & \frac{-m_{23}}{m_{22}m_{33}-m_{23}m_{32}} \end{bmatrix}\begin{bmatrix} k_1 & 0 \\ 0 & k_3e^{-aU^2} \\ t_1k_1 & t_3k_3e^{-aU^2} \end{bmatrix} \\ &= \begin{bmatrix} \frac{k_1}{m_{11}} & 0 \\ -\frac{m_{23}}{m_{22}m_{33}-m_{23}m_{32}}t_1k_1 & -\frac{m_{33}+m_{23}t_3}{m_{22}m_{33}-m_{23}m_{32}}k_3e^{-aU^2} \end{bmatrix}\end{aligned} \tag{44}$$

$$\mathbf{n}_f(\boldsymbol{\nu}) = \mathbf{\Pi M}^{-1}(\mathbf{R}^T\hat{\mathbf{e}}-\mathbf{n}(\boldsymbol{\nu})) \tag{45}$$

Here $\mathbf{M} = \{m_{ij}\}$. The ship model and the bow thruster satisfy the following properties:

$$k_1, k_3 > 0 \tag{46}$$

$$m_{11}, m_{22,}m_{33} > 0 \tag{47}$$

$$m_{22}m_{33} - m_{23}m_{32} > 0 \tag{48}$$

$$t_3 > 0 \tag{49}$$

Using the fact that $0 \leq |m_{23}| < m_{33}$, the matrix $\mathbf{B}_f$ is invertible if:

$$m_{33} + t_3m_{23} > 0 \tag{50}$$

This is the true when the length of the tunnel thruster arm t_3 satisfies the constraint:

$$t_3 > \frac{m_{33}}{-m_{23}} \tag{51}$$

where both m_{23} and m_{33} depend on the speed U and the wave frequency of encounter ω_e. The constraint (51) has a physical interpretation since the off-diagonal element $(-m_{23})$, which is recognized as the *product of inertia*, multiplied with the *tunnel thruster arm* (t_3), must be larger than

the *moment of inertia* (m_{33}), if the bow of the ship is to be moved transverse (sway direction) to generate a yaw moment.

The control law is computed from the input mapping (43) assuming (51) is true, that is:

$$\begin{aligned} \mathbf{u} &= \mathbf{B}_f^{-1}(\mathbf{f} - \mathbf{n}_f) \\ &= \mathbf{B}_f^{-1}(\mathbf{f} - \mathbf{\Pi}\mathbf{M}^{-1}(\mathbf{R}^T\hat{\mathbf{e}} - \mathbf{n})) \end{aligned} \tag{52}$$

where:

$$\begin{aligned} \mathbf{f} &= -\mathbf{R}_\pi^T\mathbf{P}_1^{-1}\mathbf{P}_2^{-1}(\mathbf{C}_2\mathbf{z}_2 + (\mathbf{z}_1 + \mathbf{P}_2\mathbf{C}_1(\mathbf{\Pi}\mathbf{R}\boldsymbol{\nu} - \dot{\mathbf{p}}_d)) \\ &\quad +\mathbf{R}_\pi^T(\ddot{\mathbf{p}}_d - \mathbf{\Pi}\dot{\mathbf{R}}\boldsymbol{\nu}) \end{aligned} \tag{53}$$

Here $\mathbf{C}_2 = \mathbf{C}_2^T > 0$ is a design matrix. Hence

$$\dot{V}_2 = -\mathbf{z}_1^T\mathbf{C}_1\mathbf{z}_1 - \mathbf{z}_2^T\mathbf{C}_2\mathbf{z}_2 \leq 0 \tag{54}$$

Theorem 3 (Degraded Tracking) *The nonlinear system (12) and (32) with control law (52)–(53) and disturbance adaptation law (41) is stable for smooth reference trajectories* $\mathbf{p}_d, \dot{\mathbf{p}}_d, \ddot{\mathbf{p}}_d \in L_\infty$ *if the rudder arm satisfies (51) and the internal dynamics are stable under Conjecture 2. Tracking of position follows from* $\mathbf{z}_1 = \mathbf{p} - \mathbf{p}_d \to \mathbf{0}$, *and tracking of velocity* $\dot{\mathbf{p}} - \dot{\mathbf{p}}_d \to \mathbf{0}$ *follows from* $\mathbf{z}_2 = \mathbf{C_1}\mathbf{z_1} + \mathbf{P_1}(\mathbf{\Pi}\mathbf{R}\boldsymbol{\nu} - \dot{\mathbf{p}}_\mathbf{d}) \to \mathbf{0}$.

Proof. The dynamics in the new variables is given by

$$\begin{bmatrix} \dot{\mathbf{z}}_1 \\ \dot{\mathbf{z}}_2 \end{bmatrix} = -\begin{bmatrix} \mathbf{P}_1^{-1}\mathbf{C}_1 & -\mathbf{P}_1^{-1} \\ \mathbf{P}_2^{-1} & \mathbf{P}_2^{-1}\mathbf{C}_2 \end{bmatrix}\begin{bmatrix} \mathbf{z}_1 \\ \mathbf{z}_2 \end{bmatrix} + \begin{bmatrix} \mathbf{0} \\ -\mathbf{P}_1\mathbf{\Pi}\mathbf{R}\mathbf{M}^{-1}(U)\mathbf{R}^T \end{bmatrix}\tilde{\mathbf{e}} \tag{55}$$

$$\dot{\tilde{\mathbf{e}}} = \mathbf{\Gamma}\mathbf{R}\mathbf{M}^{-T}(U)\mathbf{R}^T\mathbf{\Pi}^T\mathbf{P}_1\mathbf{P}_2\mathbf{z}_2 \tag{56}$$

Boundedness and stability of $(\mathbf{z}_1, \mathbf{z}_2, \tilde{\mathbf{e}})$ follow directly from a positive definite V_2 (39) and $\dot{V}_2 \leq 0$ (54). Hence with $\ddot{V}_2$ bounded, convergence of $\dot{V}_2 \to 0$ and then also convergence of $\mathbf{z}_1$ and $\mathbf{z}_2$ to the origin follow from Barbalat's lemma. Convergence of $\mathbf{z}_1$ and $\mathbf{z}_2$ to the origin implies that $\mathbf{p} \to \mathbf{p}_d$, i.e. tracking of the desired trajectory is accomplished. The stability properties rely on stable zero dynamics, which is consistent with Conjecture 2. GUAS cannot be established here, since the rank of the regressor matrix is reduced: rank $\left(\mathbf{\Gamma}\mathbf{R}\mathbf{M}^{-T}(U)\mathbf{R}^T\mathbf{\Pi}^T\mathbf{P}_1\mathbf{P}_2\right) = 2 < 3$.

4.1 Internal dynamics

The degraded control law does not stabilize the yaw angle and the yaw rate directly, and hence they are referred to as internal states. The internal dynamics can be unstable for some ships. The stability of the internal dynamics depends mainly on the damping terms in yaw. Situations may occur where these are not large enough to stabilize the yaw rate, and the ship may turn 180 degrees and continue backwards. A solution to this problem is to introduce a so-called virtual reference point (introduced by Lindegaard [15]). Then some point ahead of the ship is tracked instead of the center of rotation. The yaw dynamics is then proven to be stabilizable.

4.2 Case Study: Supply Vessel

The degraded tracking control law was simulated on the supply vessel given in Appendix A. The *non-dimensional* design parameters were selected by trial and failure to be: $\mathbf{P}_1'' = 10 \cdot \mathbf{I}$, $\mathbf{P}_2'' = \mathbf{I}$, $\mathbf{C}_1'' = \mathbf{C}_2'' = \mathbf{I}, \mathbf{\Gamma}''$=$0.05 \cdot \mathbf{I}$. The disturbance is in this case also given by a constant in the y-direction: $\mathbf{e}''$=$5 \cdot 10^4[0,\ 1/mg, 0]^T$. The time responses for the same trajectory with desired speed $1.0m/s$ and $\Delta = 0.2s$ are shown in Figures 7-11. Convergence in position is obtained and the yaw rate is seen to be bounded. Notice also that the estimated environmental disturbances are bounded as expected. The deviation between desired heading, that is the heading along the desired position trajectory, and the true heading varies more in the degraded case than in the overactuated case, since heading here is not controlled directly. It is however seen that for this simulation, the ship does not turn around 180 degrees, and the internal states (yaw and yaw rate) are bounded as assumed in Conjecture 2. The offset in the heading angle when going East and West (see e.g. for time 2200 sec to 2700 sec) is due to the environmental disturbance that is counteracted, when the disturbance comes from the side of the ship.

5 Conclusions

In this paper, nonlinear tracking control laws for ships have been derived by using adaptive backstepping techniques. Emphasis has been placed on nonlinear ship models incorporating the effect of hydrodynamic effects due to time-varying speed and wave frequency. Two cases have been addressed. In the first case ship tracking with full actuation in surge, sway, and yaw has been discussed. The second case demonstrates an emergency situation where only one of the main propellers and the bow thruster are available for tracking control. Slowly-varying environmental disturbances due to ocean currents, 2nd-order wave drift and wind forces are compensated for by using parameter adaptation. Global uniform asymptotic stability has been proven in the case of tracking control for an overactuated vessel, whereas tracking of position and linear velocity has been proven for the degraded control case. Finally, computer simulations demonstrate the performance of the control laws.

Acknowledgments

The authors are grateful to Karl-Petter Lindegaard and the reviewers for valuable comments. The work was partially financed by a grant to the third author from Kværner ASA and The Research Council of Norway.

Appendix

A Speed Dependent Model of a Supply Vessel

A speed dependent model of a supply vessel with length $L = 76.2$ (m) can be derived from the data set of Fossen et al. [4]. The ship model is identified from sea trials performed at constant speed $U_0 = 0.2\ m/s$ in calm water. The non-dimensional model in surge, sway, and yaw is given by:

$$\mathbf{M}''\dot{\boldsymbol{\nu}}''+\mathbf{N}''(U_0)\boldsymbol{\nu}''= \boldsymbol{\tau}'' \tag{57}$$

Bis-scaled values			SI-units		
U_0''	=	0.00586	U_0	=	0.2 (m/s)
L''	=	1.0	L	=	76.2 (m)
m''	=	1.0	m	=	$4.0 \cdot 10^6$ (kg)
I_z''	=	0.09	I_z	=	$2.0903 \cdot 10^9$ (kgm^2)
x_G''	=	0.0	x_G	=	0.0 (m)
$X_{\dot{u}}''$	=	-0.1274	$X_{\dot{u}}$	=	$-0.5096 \cdot 10^6$ (kg)
$Y_{\dot{v}}''$	=	-0.8902	$Y_{\dot{v}}$	=	$-3.5608 \cdot 10^6$ (kg)
$Y_{\dot{r}}''$	=	-0.0744	$Y_{\dot{r}}$	=	$-0.02268 \cdot 10^9$ (kgm)
$N_{\dot{v}}''$	=	-0.0744	$N_{\dot{v}}$	=	$-0.02268 \cdot 10^9$ (kgm)
$N_{\dot{r}}''$	=	-0.0378	$N_{\dot{r}}$	=	$-0.8780 \cdot 10^9$ (kgm^2)
X_u''	=	-0.0358	X_u	=	$-0.05138 \cdot 10^6$ (kg/s)
Y_v''	=	-0.1183	Y_v	=	$-0.1698 \cdot 10^6$ (kg/s)
Y_r''	=	0.01379	Y_r	=	$1.5081 \cdot 10^6$ (kgm/s)
N_r''	=	-0.03036	N_r	=	$-0.2530 \cdot 10^9$ (kgm^2/s)

Table 1: Model parameters of the supply vessel.

where $\mathbf{M}''$ and $\mathbf{N}'' = \mathbf{C}'' + \mathbf{D}''$ are *Bis-scaled* matrices given by:

$$\mathbf{M}''= = \begin{bmatrix} 1.1274 & 0 & 0 \\ 0 & 1.8902 & -0.0744 \\ 0 & -0.0744 & 0.1278 \end{bmatrix} \tag{58}$$

$$\mathbf{N}''(U_0) = \left\{ n_{ij}'' \right\} = \begin{bmatrix} 0.0358 & 0 & 0 \\ 0 & 0.1183 & -0.0124 \\ 0 & -0.0041 & 0.0308 \end{bmatrix} \tag{59}$$

Here U_0 is the speed used in the experiments. Calm water implies that $\omega_e \to \infty$. Hence, the expressions for $\mathbf{M}(U), \mathbf{C}(\boldsymbol{\nu})$ and $\mathbf{D}(U)$ can be derived from (see [2] for notation details):

$$\mathbf{M} = \mathbf{M}_{RB} + \mathbf{M}_{A0} = \begin{bmatrix} m - X_{\dot{u}} & 0 & 0 \\ 0 & m - Y_{\dot{v}} & mx_G - Y_{\dot{r}} \\ 0 & mx_G - Y_{\dot{r}} & I_z - N_{\dot{r}} \end{bmatrix} \tag{60}$$

$$\mathbf{N}(U_0) = \begin{bmatrix} -X_u & 0 & 0 \\ 0 & -Y_v & (m - X_{\dot{u}} + Y_{\dot{v}})U_0 - Y_r \\ 0 & (X_{\dot{u}} - 2Y_{\dot{v}})U_0 - Y_r & (mx_G - Y_{\dot{r}})U_0 - N_r \end{bmatrix} \tag{61}$$

After some manipulations, the following formulas are obtained with $x_G = 0$:

$$X_{\dot{u}}'' = 1 - m_{11}'' = -0.1274 \tag{62}$$

$$Y_{\dot{v}}'' = 1 - m_{22}'' = -0.8902 \tag{63}$$

$$Y_{\dot{r}}'' = m_{23}'' = m_{32}'' = -0.0744 \tag{64}$$

$$(I_z - N_{\dot{r}})'' = m_{33}'' = 0.1278 \tag{65}$$

Hence:

$$U_0'' = \frac{n_{23}'' - n_{32}''}{(1 - 2X_{\dot{u}}'' + 3Y_{\dot{v}}'')} = 0.00586 \tag{66}$$

$$Y_r'' = (1 - X_{\dot{u}}'' + Y_{\dot{v}}'')U_0'' - n_{23}'' = 0.01379 \tag{67}$$

$$N_r'' = (m''x_G'' - Y_{\dot{r}}'')U_0'' - n_{33}'' = -0.03036 \tag{68}$$

The resulting *Bis-scaled* values and corresponding dimensional quantities are shown in Table 1.

A suitable quadratic damping matrix

$$\mathbf{D}_M''(\boldsymbol{\nu}'') = \begin{bmatrix} 1.3\,|u''| & 0 & 0 \\ 0 & 25.0\,|v''| & -10.0\,|r''| \\ 0 & -10.0\,|v''| & 5.0\,|r''| \end{bmatrix} \tag{69}$$

was derived by assuming that the velocities are bounded by

$$|u| \leq 4\,m/s,\ \ |v| \leq 1\,m/s,\ \ |r| \leq 1\ \mathrm{deg}/s$$

The control configuration matrix is given by (Bis scaled):

$$\mathbf{T}''= \begin{bmatrix} 1 & 1 & 0 & 0 & 0 \\ 0 & 0 & 1 & -1 & -1 \\ 5/L & -5/L & 60/L & 38/L & 38/L \end{bmatrix} \tag{70}$$

The force coefficients and the control allocation weights were chosen as:

$$\begin{aligned} \mathbf{K}'' = \frac{1}{mg}\mathrm{diag}\Big\{ & 6.55 \cdot 10^5, 6.55 \cdot 10^5, 1.37 \cdot 10^5 \cdot e^{-47 \cdot (U'')^2}, \\ & 3.9 \cdot 10^5 + 6.4 \cdot 10^8 \cdot (U'')^2, 3.9 \cdot 10^5 + 6.4 \cdot 10^8 \cdot (U'')^2 \Big\} \end{aligned} \tag{71}$$

$$\mathbf{W}''=\mathrm{diag}\left\{1, 1, 0.25 \cdot (1 + e^{200 \cdot (U'')^2}), 2.5 \cdot 10^{-8} \cdot e^{\frac{1}{0.02 + 0.6U''}}, 2.5 \cdot 10^{-8} \cdot e^{\frac{1}{0.02 + 0.6U''}}\right\} \tag{72}$$

References

[1] **Berge, S. P. and T. I. Fossen.** On the Structural Properties of the Nonlinear Ship Equations of Motion Incorporating the Effects of Forward Speed, *Submitted to the International Journal of Mathematical Modelling of Systems*, 1998.

[2] **Fossen, T. I.** Guidance and Control of Ocean Vehicles, *John Wiley & Sons Ltd*, 1994.

[3] **Fossen, T. I. and O.-E. Fjellstad**. Nonlinear Modelling of Marine Vehicles in 6 Degrees of Freedom, *International Journal of Mathematical Modelling of Systems,* **JMMS-1**(1):17–28, 1995.

[4] **Fossen, T. I, S. I. Sagatun and A. J. Sørensen.** Identification of Dynamically Positioned Ships, *Journal of Control Engineering Practice,* **CEP-4**(3):369–376, 1996.

[5] **Fossen, T. I. and A. Teel.** UGAS/ULES when backstepping with integral action: Applications to Mechanical Systems and Ships, *Submitted to the International Journal of Robust and Nonlinear Control*, 1998.

[6] **Fossen, T. I. and J. P. Strand.** Passive Nonlinear Observer Design for Ships Using Lyapunov Methods: Experimental Results with a Supply Vessel, *Automatica,* **AUT-35**(1), January 1999.

[7] **Fossen, T. I., J.- M. Godhavn, S. P. Berge, and K. - P. Lindegaard.** Nonlinear Control of Underactuated Ships with Forward Speed Compensation, *Proc. of the IFAC Workshop on Nonlinear Control Systems (NOLCOS'98)*, The Netherlands, 1998.

[8] **Fossen, T. I. and S. P. Berge,** Nonlinear Vectorial Backstepping Design for Global Exponential Tracking of Marine Vessels in the Presence of Actuator Dynamics, *Proceedings of IEEE Conference on Decission and Control (CDC'97)*, San Diego, pp. 4237-4242, December 1997.

[9] **Fossen, T. I. and Å. Grøvlen.** Nonlinear Output Feedback Control of Dynamically Positioned Ships Using Vectorial Observer Backstepping, *IEEE Transactions on Control Systems Technology,* **TCST-6**(1):121–128, January 1998.

[10] **Godhavn, J.- M.** Nonlinear Tracking of Underactuated Surface Vessels, *Proc. of the 36th IEEE Conference on Decision and Control (CDC'96)*, Kobe, Japan, pp. 975–981, 1996.

[11] **Godhavn, J.- M.** Topics in Nonlinear Motion Control - Nonholonomic, Underactuated, and Hybrid Systems, Dr. Ing. Thesis, *Department of Engineering Cybernetics, The Norwegian University of Science and Technology*, 1997.

[12] **Husa, K. E. and T. I. Fossen**. Backstepping Designs for Nonlinear Way-Point Tracking of Ships. *Proc. of the 4th IFAC Conference on Manoeuvering and Control of Marine Craft, Brijuni, Croatia,* 10-12 September, 1997.

[13] **Krstic M., I. Kanellakopoulos and P. Kokotovic.** Nonlinear and Adaptive Control Design, *John Wiley & Sons Inc,* 1995.

[14] **Krstic M., I.** Invariant Manifolds and Asymptotic Properties of Adaptive Nonlinear Stabilizers, *IEEE Transactions on Automatic Control,* **TAC-41**(6):817-829, 1996.

[15] **Lindegaard K.,-P.** Nonlinear Tracking Control and Station-Keeping of Underactuated Ships, MsC thesis, *Department of Engineering Cybernetics, Norwegian University of Science and Technology*, 1997. (Short version will be submitted to IEEE TCST 1998).

[16] **Salvesen, N., E. O. Tuck and O. Faltinsen.** Ship Motions and Sea Loads, *Annual Meeting of The Society of Naval Architects and Marine Engineers (SNAME)*, New York, November 12-13, 1970 (also published by: Det norske Veritas (DnV), Publication 75, vol. 6, pp. 1–30, 1971).

[17] **SNAME (The Society of Naval Architects and Marine Engineers).** Nomenclature for Treating the Motion of a Submerged Body through a Fluid, *Technical and Research Bulletin No. 1-5,* 1950.

[18] **Vik, B. and T. I. Fossen.** Semiglobal Exponential Output Feedback Control of Ships, *IEEE Transactions on Control Systems Technology,* **TCST-5**(3):360–370, 1997.

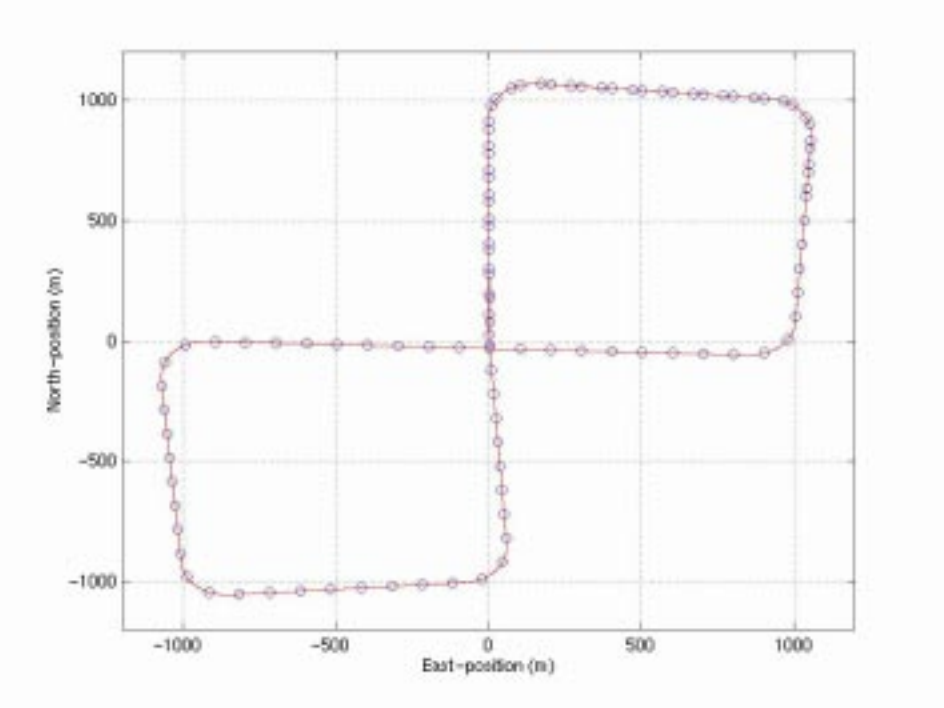

Figure 2: Overactuated control of supply vessel. The desired trajectory (solid) and the resulting trajectory (circles) are shown.

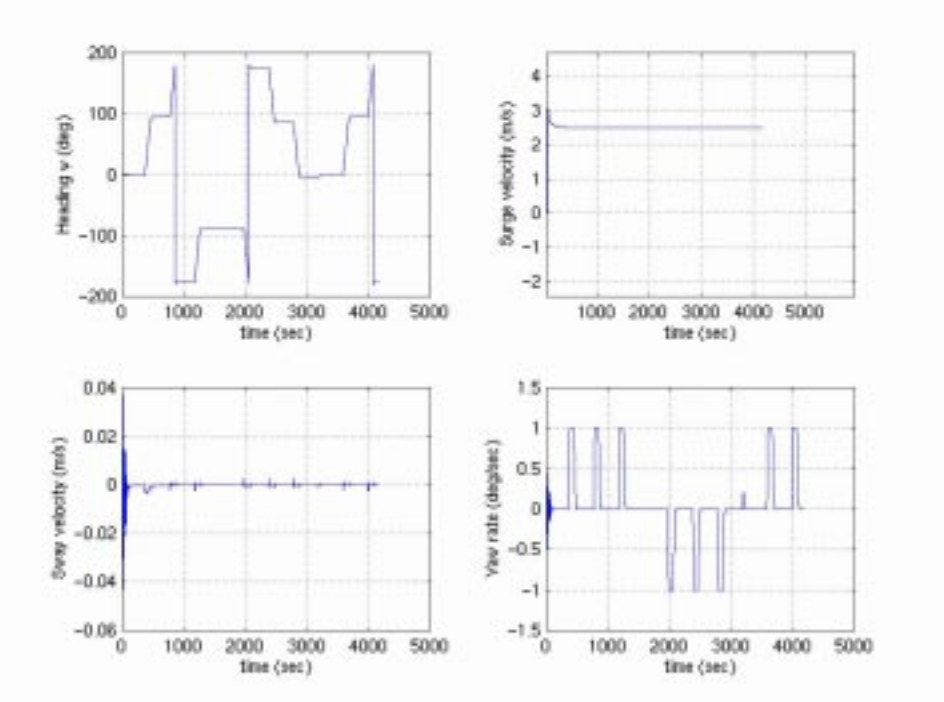

Figure 3: This figure shows the resulting heading, and the velocites in surge, sway and yaw for the overactuated control of a supply vessel.

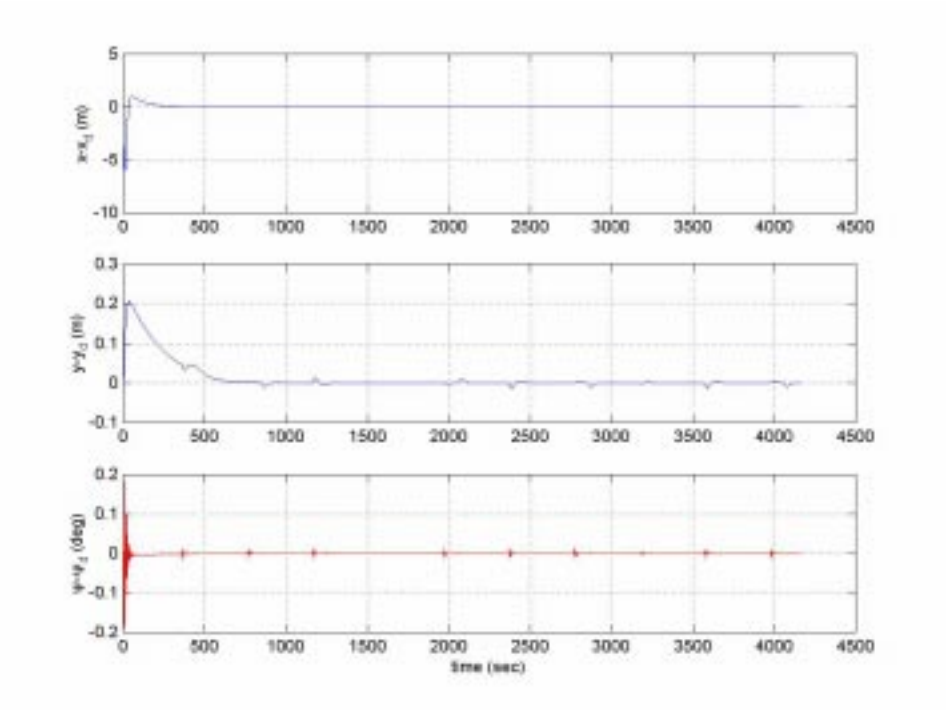

Figure 4: This figure shows that the position error and the heading deviation (tracking error) converge to zero for the overactuated control of the supply vessel.

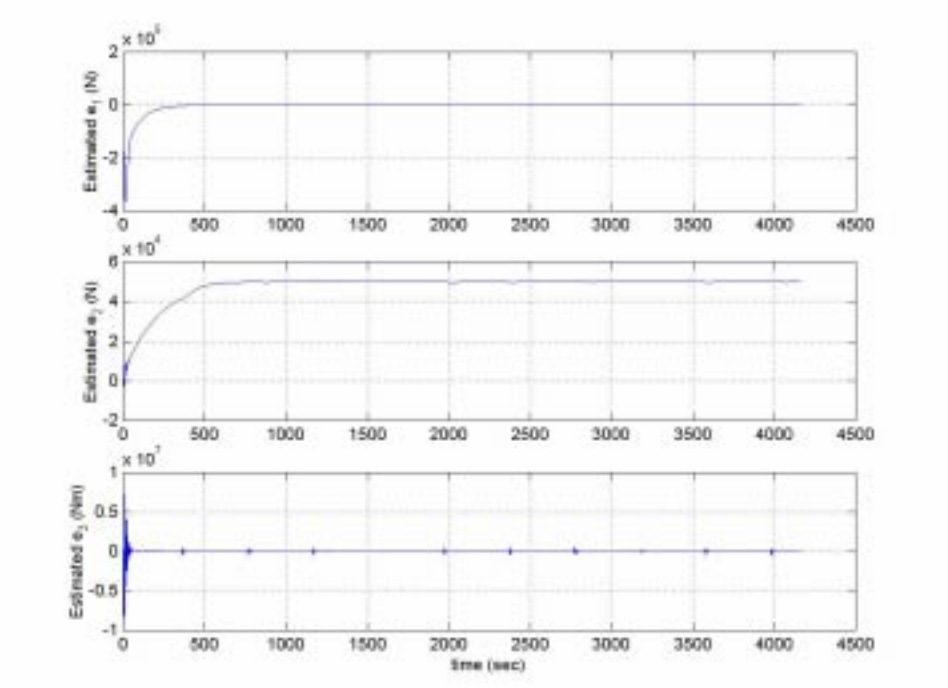

Figure 5: The estimated environmental disturbances converge to the true value in the case of overactuated control of a supply vessel.

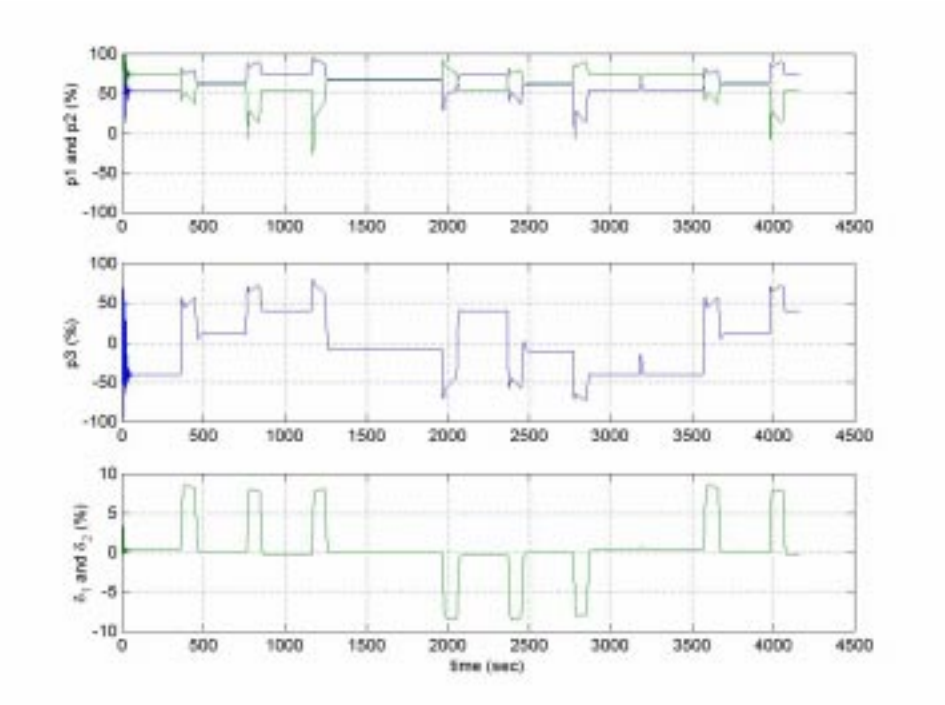

Figure 6: This figure shows how the aft propellers are used in the overactuated tracking control law for the supply vessel. The tunnel thruster is used in the turns together with the rudders.

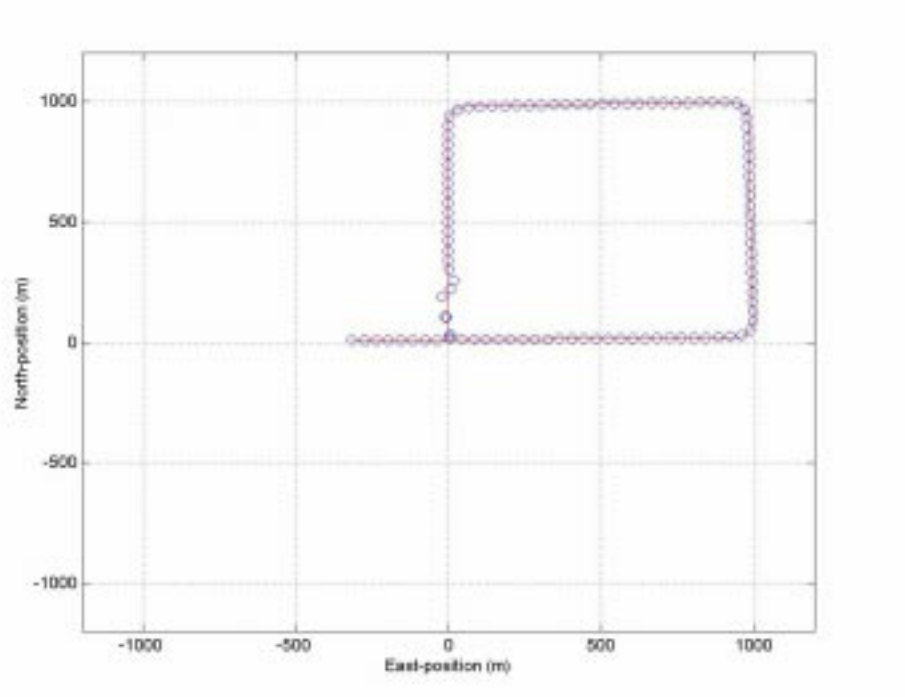

Figure 7: The trajectory for the degraded tracking control of the supply vessel is shown in this figure. The ship (circles) follows the desired trajectory (solid) well.

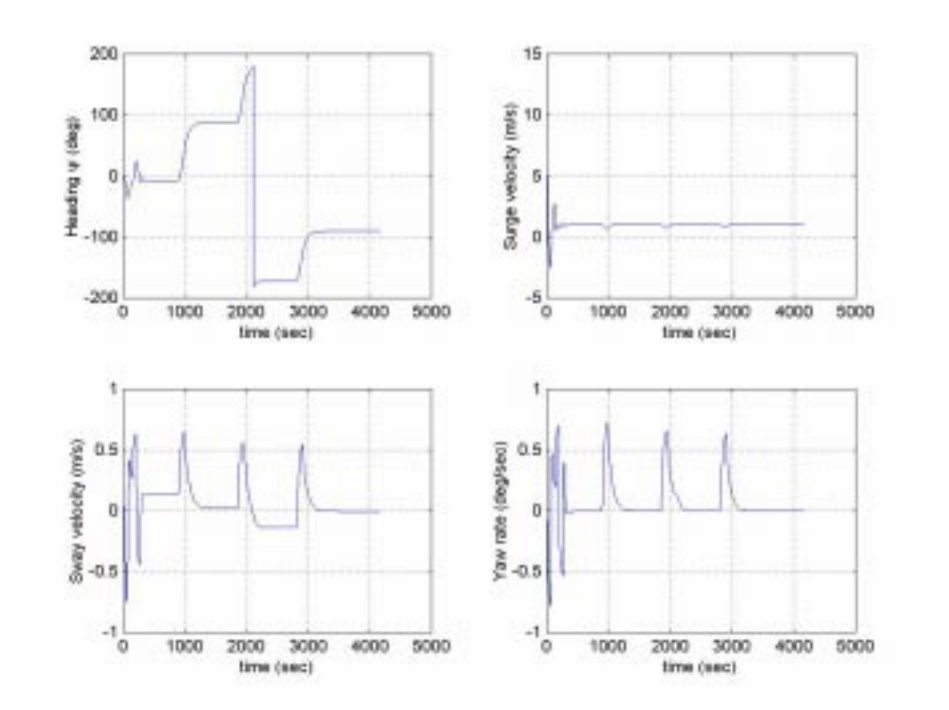

Figure 8: The degraded tracking control gives the heading angle and the velocities shown above. The sway velocity and the yaw rate increase in the turns when two controls are available.

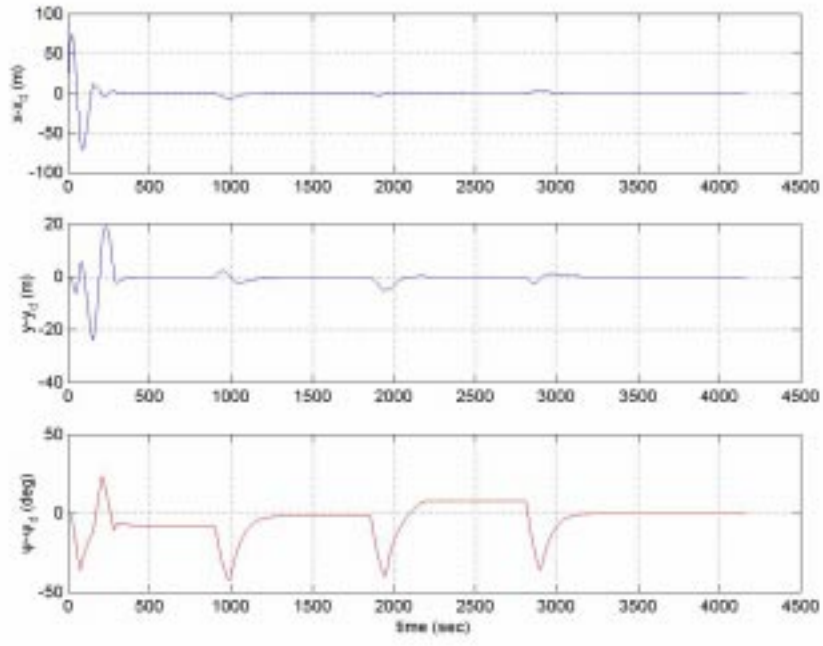

Figure 9: The figure shows that the position errors converge to zero also in the underactuated case. The heading error is in this case not controlled directly. It is however seen that it is bounded.

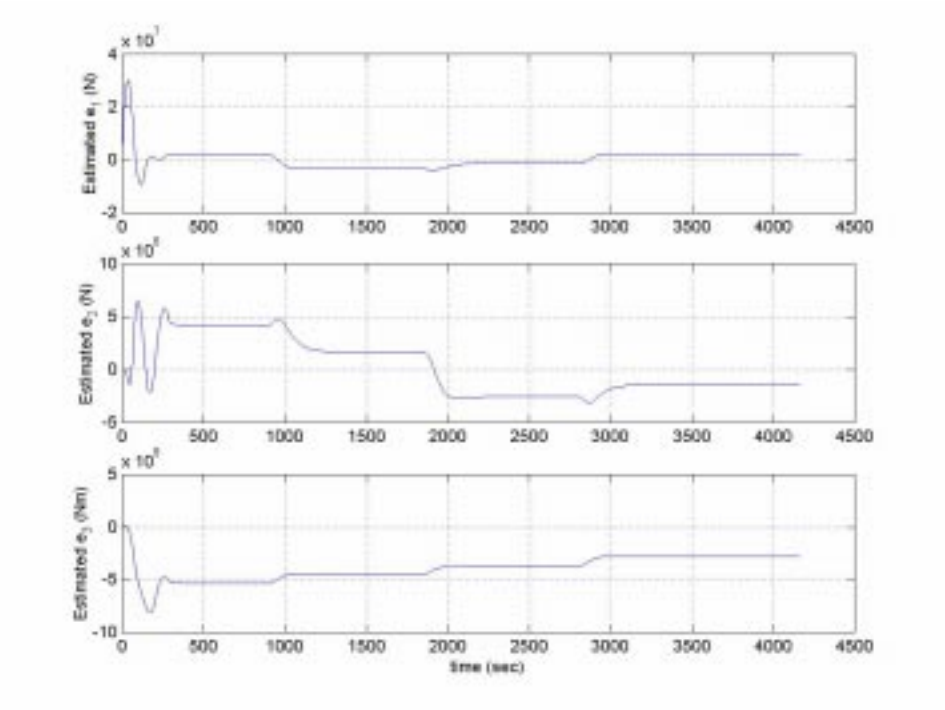

Figure 10: The estimated environmental disturbances do not converge to the true value in the underactuated case. They are however bounded.

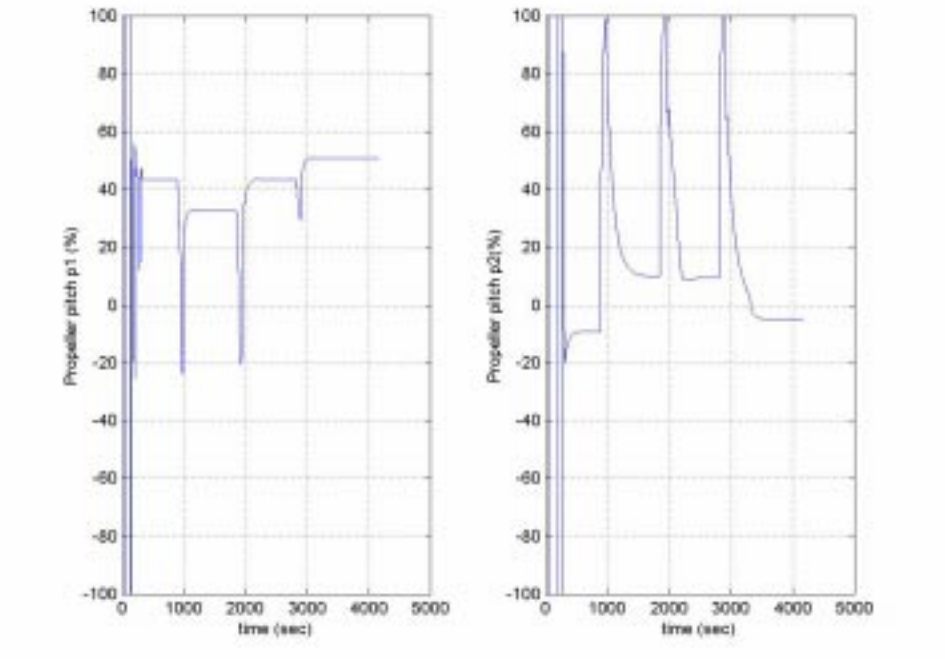

Figure 11: The figure shows how the aft propeller and the tunnel thruster are used in the degraded tracking control law.